

Chapter 4

The model

4.1 Introduction

As shown in chapter three within the review of contemporary models, for this scale of study, finite element schemes are too complex, cross sectional methods too simple and existing landscape evolution models too coarse. Thus, it seems a cellular framework is ideal, but operating at a medium resolution of 1-3m which is fine enough to allow the channel to span several cells instead of operating within one, generating a more detailed fluvial representation as of Murray and Paola (1994, 1997). This resolution may also allow representation of different grainsizes, thus allowing armouring and stratigraphies to develop. At this scale, high-powered workstations should allow slope, vegetative and hydrological processes to operate within the same framework for an area representing a small catchment (up to 10km²). From the model aims outlined and expanded in chapters 1,2 and 3, a set of more explicit specifications were draw up, from which a model could be designed.

1. The model should represent a complete catchment, avoiding concentrating only on certain cross sections or reaches.
2. Fluvial processes are potentially the most important and therefore should be represented as accurately as possible.
3. Temperate slope processes such as soil creep and mass movement should be fully integrated.
4. Vegetation influences on both the hydrology and strength of surface must be explicitly modelled.
5. A modular programming structure should be used, to allow the latter integration of different schemes, for example semi-arid slope processes.
6. A generic strategy is essential, so that the model is not site specific and can be easily adapted to operate over a variety of catchments and environments.

These aims are ambitious, and there are many refinements and optimisations made to allow the model operate over its intended time and space scales. This chapter describes a summary of its structure, operation and results of checks and validation tests.

4.2 Model description

4.2.1 Model structure

The concept and structure of this cellular automaton model is simple, but its operation complex (section 3.5.1).

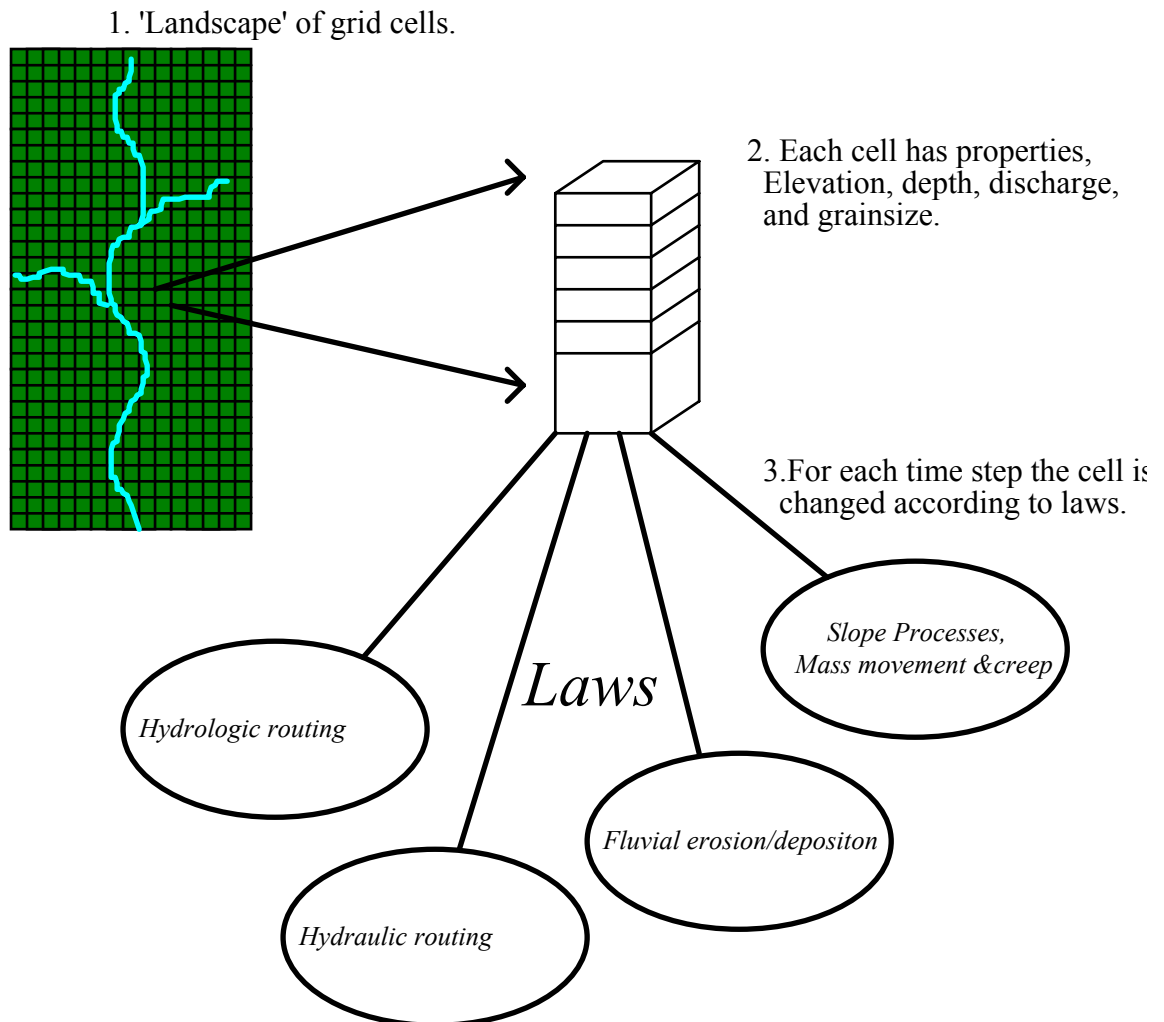


Figure 4.1. Schematic diagram of the key processes operating in the CA model.

As detailed in Figure 4.1, the catchment is represented by an array of uniform square grid cells. Each grid cell is then assigned initial values for elevation, water discharge, water depth, drainage area and grainsize fractions. For each timestep or iteration, these values are updated in relation to the immediate neighbours according to laws applied to every cell. These laws fall into four groups covering hydrological, hydraulic, erosion and slope process modelling. These four groups are discussed in the following sections. All units are in metres unless specified otherwise.

4.2.2 Hydrological model

For every minute of the model's run, the soil saturation for an individual cell (J_t) is calculated. The saturation for the next time-step (T , here 60 seconds) is then calculated (J_{t+1}), but for this an additional parameter is carried over, j_t which before each calculation is set to the previous iterations j_{t+1} . Then, if the rainfall rate (r) equals 0, J_{t+1} is calculated according to equation 4.1.

$$j_{t+1} = \frac{J_t}{1 + \left(\frac{j T}{m}\right)} \quad (4.1)$$

$$J_{t+1} = \frac{m}{T} \log\left(1 + \left(\frac{j_t T}{m}\right)\right)$$

If rainfall is not equal to 0, equation 4.2 is used.

$$j_{t+1} = \frac{r}{\left(\frac{r - j_t}{j_t} \exp\left(\left(\frac{(0 - r)T}{m}\right) + 1\right)\right)}$$

$$J_{t+1} = \frac{m}{T} \log\left(\frac{(r - j_t) + j_t \exp\left(\frac{rT}{m}\right)}{r}\right) \quad (4.2)$$

Within these expressions, m is the key variable, controlling the rise and fall of the soil moisture deficit, effectively the exponential soil water parameter in TOPMODEL (Beven and Kirkby, 1979). The runoff is multiplied by the grid cell size to obtain discharges which is added to every cell or to the margins as discussed in 4.3.2. If runoff calculations are required between these two time steps values are interpolated linearly.

4.2.3 Flow routing

For each grid cell, a runoff threshold is calculated (Equation 4.3) which is based upon the amount of water that will infiltrate through the soil, a balance of the hydraulic conductivity (K), the slope (S) and the horizontal spacing (Dx).

$$\text{Threshold} = KS(Dx)^2 \quad (4.3)$$

This is then subtracted from the soil saturation produced from equations 4.1 and 4.2 and the proportion above is treated as run off, that below as subsurface flow. This subsurface flow is routed using a multiple flow algorithm as described by Desmet and Govers (1996) (Equation 4.4).

$$Q_i = Q_o \frac{S_n^x}{\sum S_i^x} \quad (4.4)$$

Here Q_i is the fraction of discharge delivered to the neighbouring cell i from the total cell discharge (Q_o) in m^3/s^{-1} , according to the slope S between the cell and its relative neighbours I , numbering from $I-x$ (x ranging from 3 to 8 depending on the number of neighbours). With surface flow, the depth is calculated using Manning's equation (equation 4.5).

$$Q = \frac{A(R^{0.67} S^{0.5})}{n} \quad (4.5)$$

Where A is cross sectional area, R is hydraulic radius, S is slope and n is Mannings coefficient. If dealing with a cell 1m wide, this can be re-arranged to give equation 4.6, with width (w) as 1, leaving depth (d).

$$Q = d \left(\frac{R^{0.67} S^{0.5}}{n} \right) \quad (4.6)$$

However, in order to calculate the depth, the hydraulic radius has to be resolved. This is a difficult approximation, as what is the hydraulic radius for a grid cell or part

of a channel 1m wide? However for a rectangular/trapezoidal channel the hydraulic radius can be simplified as is equation 4.7.

$$R = \frac{A}{p} = \frac{wd}{w+2d} \quad (4.7)$$

If w is greater than d , then the $2d$ in the denominator can be ignored leaving d , as in equation 4.8.

$$R \approx \frac{dw}{w} = d \quad (4.8)$$

This means that equation 4.6 can be re-written to calculate depth as equation 4.9.

$$d = \left(\frac{Qn}{S^{0.5}} \right)^{\frac{3}{5}} \quad (4.9)$$

Excessively low slopes can result in excessive depths being calculated. To account for this, when the slope is less than 0.005, the depth is set to the same value as discharge. Three different methods of calculating the slope were tried, that of the average slope of the neighbours, that of the greatest slope of all the neighbours and the average of all positive slopes. The latter was found to be the most stable, but the model shows some sensitivity to the method of slope calculation. The routing effectiveness and consequently the distribution of water across a channel can be effected by this as is discussed later (section 4.8).

Water is then routed according to equation 4.10 where the depth of water as well as cells elevation is considered.

$$Q_i = Q_o \frac{[(e+d) - e_i]^x}{\sum [(e+d) - e_i]^x} \quad (4.10)$$

Here Q_i is the discharge routed to cell i , Q_o the total discharge from the cell, e is the elevation and d depth of water (in metres) for each neighbouring cell i . In both these expressions, differences in slope between diagonal neighbours are accounted for by

contributing cell up to the depth of the obstruction whilst the rest routed on. This process has the effect of filling hollows that the model creates with water. These hollows or sinks frequently have to be removed from DEM data (Goodchild and Mark 1987, Hutchinson 1989).

To drive the erosion laws, the maximum depth calculated after all these four scans is recorded. This procedure allows flow trapped after one iteration to be incorporated in the scan of the next iteration. This storage in corners and bends maintains a flow in the channel even around complex channel patterns and meanders. For example, with a meander sequence, water may be routed around the first corner, but be trapped by the second. However, in the next iteration, this water is still there, to be released in the next scan, and replaced by more water from upstream, allowing the continuum of flow.

Another way to visualise the whole process is to imagine covering a 3D map surface with water droplets. If these are squeezed across with a giant squeegee as per each scan, some water will remain in depressions or in the channel. If the same amount of water droplets is applied again, and scanned, the remaining water will have acted as a store in the hollows and bends, the same amount applied will be removed at the base.

This method gives very similar results to that of the conventional method, even in complex areas such as confluences, yet provides a massive time saving. It is validated at the end of this chapter.

4.2.4 Erosion/deposition

To represent the erosion and deposition of different grainsizes and the development of an armoured surface layer, an active layer system is used, similar to that of Parker (1990), Hoey and Ferguson (1994) and Toro-Escobar et al. (1996). This model, however, uses twelve active layers. One for bedload, one for the surface active layer and ten further subsurface layers. The surface active layer is defined as $2D_{90}$ with the ten layers below at $4D_{90}$. Nine grainsizes are represented from 0.004 to 1.024m in whole phi classes (-2ϕ to -10ϕ). Furthermore, the surface active layer has two additional categories representing a surface vegetative mat and bedrock.

When material is added to the top active layer, material is removed from this layer and added to the next layer down, as in equation 4.11.

$$E_i = \left(\frac{F_i^x}{\sum F_{i-n}^x} \right) (\sum F_{i-n}^x - A) \quad (4.11)$$

Here E_i is the amount removed from the top layer (x) and added to the next layer down ($x+1$) of grainsize fraction i . A represents the correct thickness of the active layer ($2D_{90}$ or $4D_{90}$). For erosion or degradation, material is moved up from the lower layers according to equation 4.12.

$$E_i = \left(\frac{F_i^{x+1}}{\sum F_{i-n}^{x+1}} \right) (A - \sum F_{i-n}^x) \quad (4.12)$$

Both these expressions propagate upwards and downwards respectively allowing the displacement of material through the active layers. Movement into the base of the bottom layer during degradation is in the proportions as defined in section 5.4 and Figure 5.8. No transfer function or filtering term is used (Hoey and Ferguson 1994, Toro-Escobar *et al.* 1996) as such a term has no temporal scaling. This scaling is necessary given the variable time step used in the models operation (4.3.2). This procedure allows the development of an armoured surface, and the storage of deposited sediment in the stratigraphy of the other ten active layers.

The amount eroded by fluvial action from cell to cell, is determined using the Einstein-Brown (1950) formulation. This was chosen, as much information is available about the local hydraulic conditions (Gomez and Church 1989) and the total load is calculated from the sum of fractions eroded. This is well suited to the nine grainsize classes and the active layer system used. The formulae use here takes the form of equation 4.13.

$$\psi = \frac{(\rho_s - \rho)D}{\rho d S} \quad (4.13)$$

Where ψ is the balance between the forces moving and restraining the particle, $\rho_s - \rho$ the relative density of the submerged sediment, D the grain size (metres), d the flow depth and S the energy slope. A dimensionless bedload transport rate ϕ is then calculated.

$$\phi = q_s \sqrt{\frac{\rho}{(\rho_s - \rho)gD^3}} \quad (4.14)$$

ϕ is then related to ψ by the relationship plotted by Einstein (1950),

$$\phi = 40(1 / \psi)^3 \quad (4.15)$$

A rearrangement of equations 4.14 and 4.15 then allows q_s , the volumetric sediment load in $\text{m}^3 \text{s}^{-1}$, to be calculated. For each grid cell, the amount in each grainsize class which can be eroded is calculated, and removed from the active layer of the cell in question, and deposited to the active layer of the downstream cell.

The grass layer is treated as a boulder of diameter 0.26m. This was calculated from field shear stress measurements carried out by Prosser (1996). Bedrock is similarly treated as being an un-erodeible boulder of 100m in size. When the turf is eroded however, it is not deposited, the model assumes it is swept away.

4.2.5 Slope processes

4.2.5.1 Mass movement

Mass movement is simply represented as an instantaneous removal process. When the slope between adjacent cells exceeds a threshold (currently 0.5) material is moved from the uphill cell to the one below until the angle is lower than the threshold. As a small slide in a cell at the base of a slope may trigger more movement uphill, the model continues to check the adjacent cells rows until there is no more movement. Where the cells border the main channel, material is transferred from active layer to active layer and the layers grainsize proportions accordingly updated. If the amount removed from the up-slope cell is greater than the active layer thickness, material from the subsurface is also added.

4.2.5.2 Soil creep

Soil creep is calculated between each cell every month of model time according to equation 4.16

$$Creep(yr^{-1}) = \frac{S0.01}{Dx} (4.16)$$

When calculated, the cells are updated simultaneously and where cells border the channel material is transferred to the active layer of the receiving cells.

4.2.6 Vegetation growth

Vegetation re-growth is simply represented in the model. It has no interactions with the hydrological model, its purpose is simply to allow a protective turf mat to develop over flood deposits. This process was considered important in the preservation of alluvial flood units. An extra fraction is added to the surface active layer to represent this turf cover. A simple linear growth model adds to this layer in monthly time steps if the cell is not under water and after ten years of uninterrupted growth, full cover will develop. If this layer is eroded, material is removed from the grass fraction and treated as if washed out of the catchment, instead of re-depositing. The addition or removal of vegetation has no effect upon the elevation of the cell, but the partial removal will allow material from underneath to become exposed and vulnerable to erosion.

4.3 Implementation

4.3.1 Preparation of data

The main requirement for the model is a high resolution DEM. Such data is frequently unavailable, as the most detailed commercially available DEM's have only a ten metre grid spacing. Therefore to construct (for example) a 1m DEM additional data has to be taken and the extra points interpolated. There are several commercial packages available for creating DEM's, but in this instance, the TOPOGRID command in ARC-INFO was used. This function is designed specifically for the interpolation of a hydrological DEM from contour data. It identifies areas of local maximum curvature and slope to create a network of streams and ridges, ensuring hydrogeomorphically correct output. After this general surface has been determined, the contour data is used in the interpolation of each cells elevation value. TOPOGRID also removes topographic sinks and hollows. This is necessary as many artificial sinks are produced by errors interpolating the DEM from contour data (Goodchild and Mark 1987, Hutchinson 1989).

The only other data required are hourly (or finer) rainfall figures and the initial grainsize distributions.

4.3.2 Run time optimisations

A 1m resolution DEM representing a 4km² catchment is complex, with over 4 million points. However for most of the model operation time, many areas are dormant, yet can at times become active. The model, therefore only needs to concentrate where there is activity, i.e. running water. This is achieved by scanning the whole catchment every 5 000 iterations, selecting the cells which have water running in them and those within a 5 cell proximity. These cells are then used for the next 5 000 iterations. This operation is fraught with complexity, since it is easy for the model to ignore a small section e.g. in the middle of the main channel, halting the flow. This procedure also has to account for the expanding dimensions of the drainage network during the passage of a flood. To combat this, the model checks to see if the channel is trying to push out of the previously selected area, if so, the area is re-scanned.

For every iteration, the hydrological input is added at the edges of this area. The amount added is determined by multiplying the output from the hydrological model by the area drained by these border cells. This drainage area is calculated using an adaptation of the 'scanning' algorithm. For the area calculation, each cell is given a value of one. This value is then 'pushed' across the whole catchment in a similar manner to that described in 4.1.3. The maximum value for each cell from all the scans is recorded, and this shows the number of cells drained by each cell. In effect it ranks each cell by its drainage capacity. When the amount is added at the edge of the selected area, a flag is initiated in the grid cell to prevent the addition of the same amount in another scan.

The net result of these operations are that for 98 to 99% of the models operating time, less than 10% cells are checked, yet periodically all of them are. This provides a substantial computational time saving of several orders of magnitude, making the operation at a catchment scale feasible.

The landslide section is optimised by checking slide conditions at each iteration only for cells in the immediate proximity of the channel. The whole catchment is then checked every 500 iterations. Creep is calculated every month in real time. This is necessary, as creep is a very slow process and if a smaller time-step is used, the amount moved on low gradients is too small for the numerical precision of the program.

For all other functions, a variable time-step is used. This is adjusted so the maximum amount that can be removed or deposited from one cell to another is a small proportion of the average slope ($< 10\%$). A maximum time step of 120 seconds is introduced allowing significantly rapid progress in low flow situations, yet not too long as to miss any part of a storm. The boundary conditions unless otherwise specified were fixed so that none of the edge cells can be altered in elevation, but material can pass over them, similar to the conditions at the outflow of a flume.

4.4 Operation

4.4.1 Spin up - initiation

With a model of this size and resolution, the definition of the initial conditions is difficult yet crucial. It is presently impossible to accurately define grainsize composition, bedrock depth and vegetation for a catchment of 4 million grid cells to a depth of two metres. Therefore the initial conditions are forced to ‘evolve’ from a set landscape. This procedure is carried out according to the following steps.

1. The DEM created from Arc-info is taken, and each cell is given a grainsize composition of the proportions described (for Cam Gill Beck) in Figure 5.8.
2. Bedrock depth is set at 1m below the surface throughout the catchment.
3. The model is then run for 200 iterations with a flood event of $3 \text{ m}^3\text{s}^{-1}$ forced down the catchment. This is carried out without a vegetation layer to allow the channel pattern to form.
4. The vegetation layer is then added to the undisturbed cells.

The catchment is then in its first initial state. Model runs can be made directly from this condition, or sets of floods can be applied, to allow the catchment to become used to a particular regime.

4.4.2 Description of model's operation

During the course of a run, the model runs through the sequence of operation shown in Figure 4.3. Initially, all the variables are set to zero, and then the initial values for elevations, grainsizes and rainfall are loaded. The model then calculates the drainage area and the region to be ‘scanned’ (4.3.2). The model then enters the main loop, starting with a calculation of the hydrological input from the rainfall data. Water is then routed and depths calculated by scanning across the catchment four times as detailed in 4.2.3. The amount eroded and deposited fluvially between cells can then be determined and cells elevation values updated. Finally ‘local’ landslides around the scanned area are calculated. Every 5000 iterations the model re checks the drainage area and scanned area, and every 500 iterations carries out a landslide routine over the whole catchment. At the end, and periodically during the simulation, final elevations and grainsizes are saved for analysis.

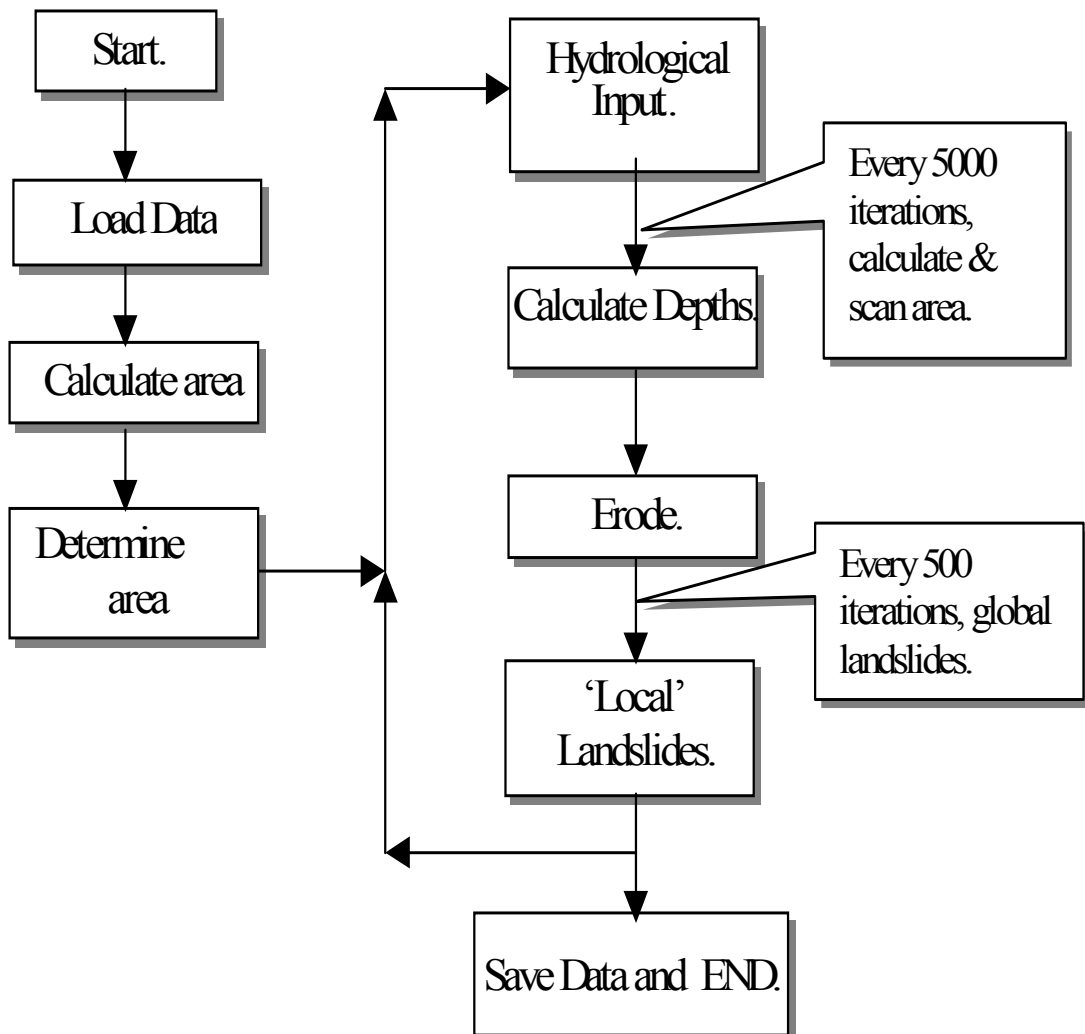


Figure 4.3 Schematic of model's operation.

4.5 Evaluation

4.5.1 Testing of flow routing

4.5.1.1 Method

To evaluate key sections of the model, several tests were derived. In the first test, erosion/deposition and mass movement sections were disabled, making the model operate as an empty flume, and known discharges applied at the top of the channel. As the channel geometry was known, the depth of water was calculated for the whole channel width from equation 4.5. These results are shown in Figure 4.4. The second test was similar but the depths were taken and the discharge calculated using the initial version of Manning's equation (4.5) over three different channels, two rectangular and one triangular. The results are shown in Figure 4.5.

Other tests were made to establish the model's competence at routing flow in channels of varying dimensions at differing discharges, in particular examining the velocity distribution and the profile of the water surface. Four scenarios were tried, a rectangular and triangular channel (Figure 4.6), a triangular channel with central obstacle i.e. a bar (Figure 4.7) and a rectangular channel with an off centre obstacle (Figure 4.8).

4.5.1.2 Discussion

Although Figure 4.4 shows the model is interpreting the adaptation of Manning's equation (4.5) into a CA framework well, Figure 4.5 gives slightly poorer results. The two rectangular channels both give good results, but the triangular worse. Figure 4.6 shows that the water surface and velocity profile is well represented in a rectangular channel, with a slight drop off in elevation near the channel edges. The triangular channel is less well depicted with the water almost 'clinging' to the edges of the bank. Figure 4.8 shows a small degree of super elevation (0.15m) down the centre fastest part of the channel. Although providing a good representation, these results reveal some inaccuracies which can be attributed to four main factors.

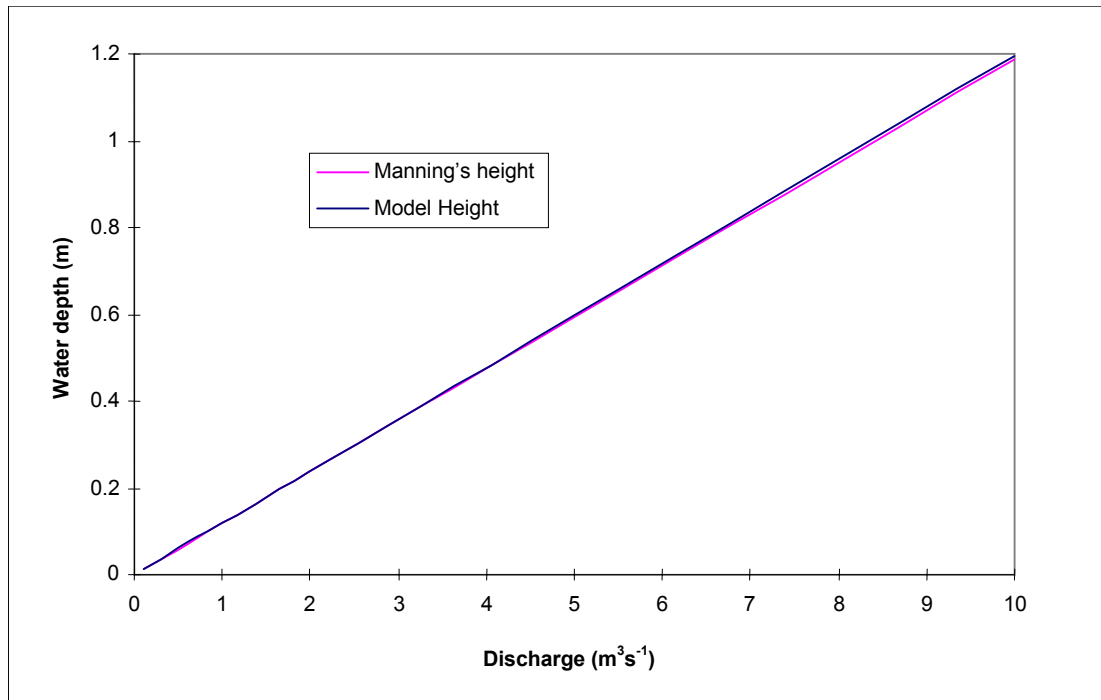


Figure 4.4. Graph showing depths calculated using the model's adaptation of Manning's formula (1.6) and the original.

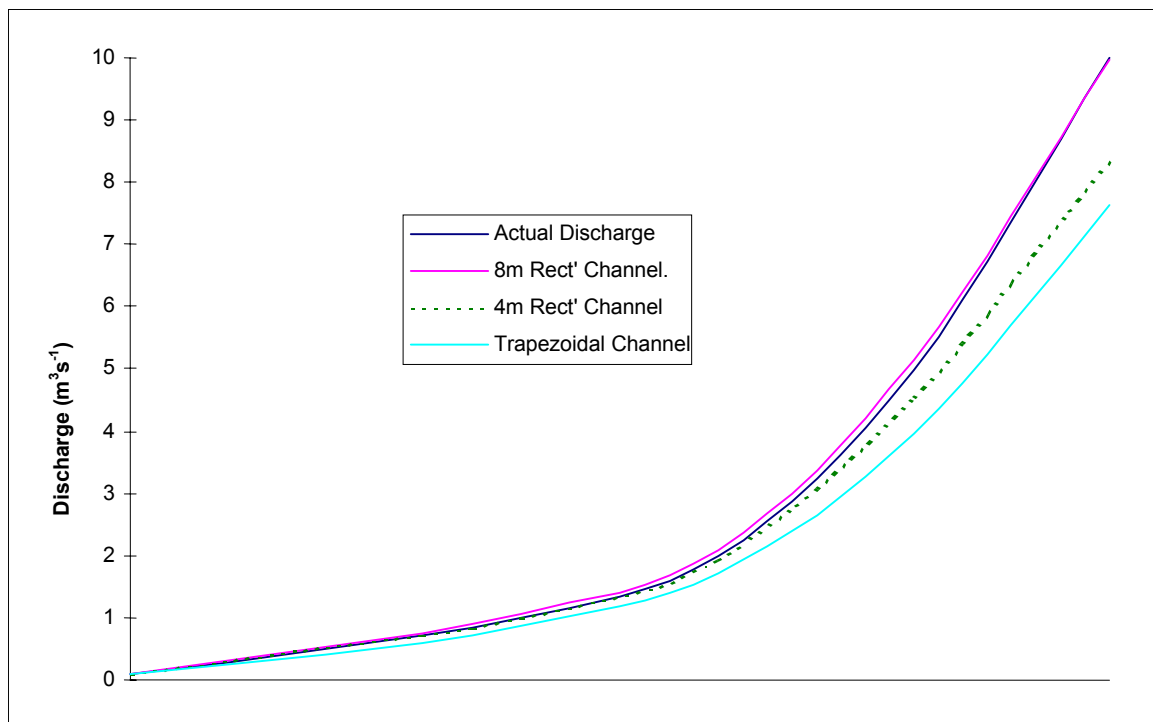


Figure 4.5. Graph showing actual discharge inputted to the model, and discharge calculated by Manning's formula (1.2), and using model outputs of depth and width.

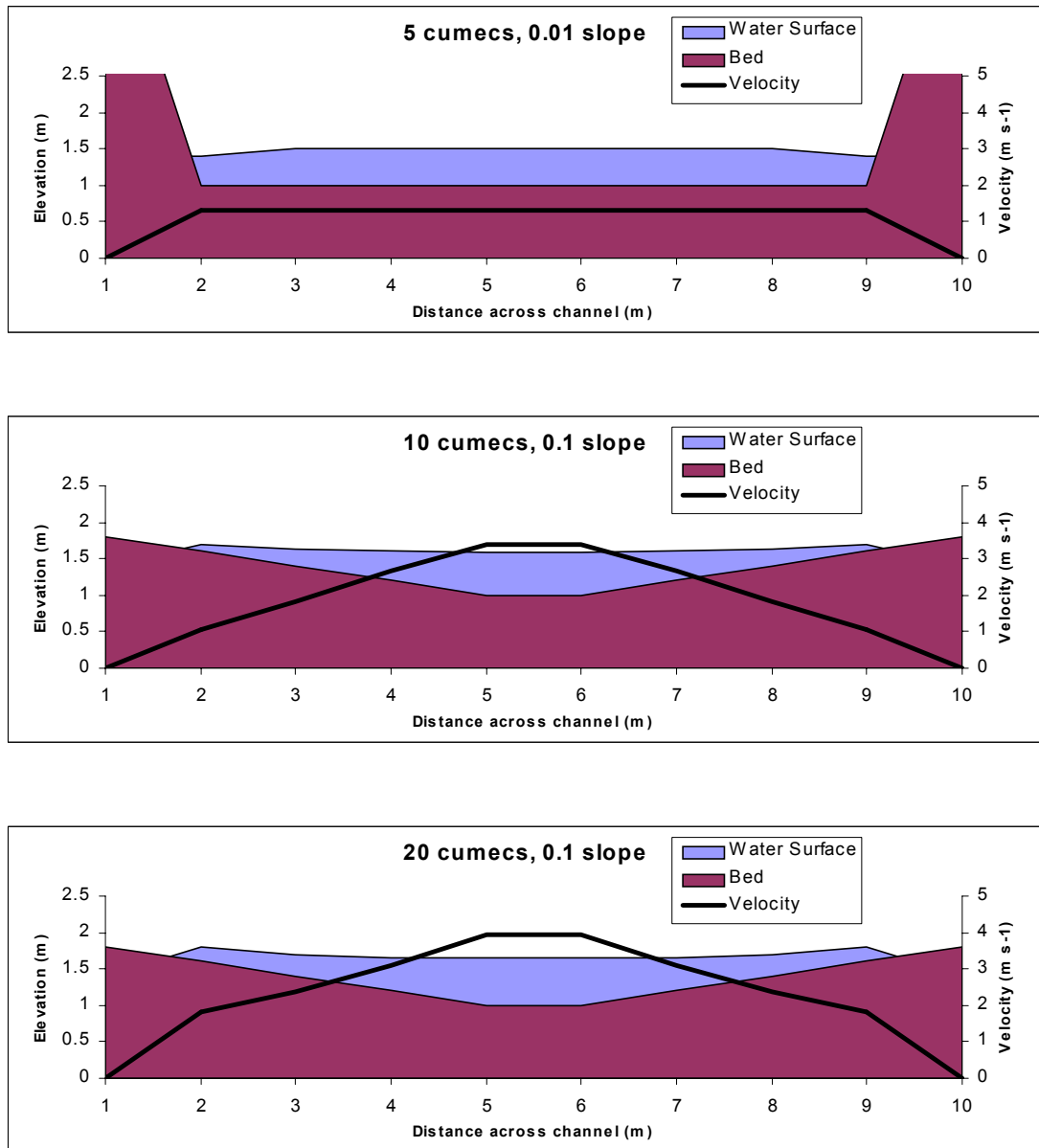


Figure 4.6. Velocity and water surface profiles for rectangular and triangular channels.

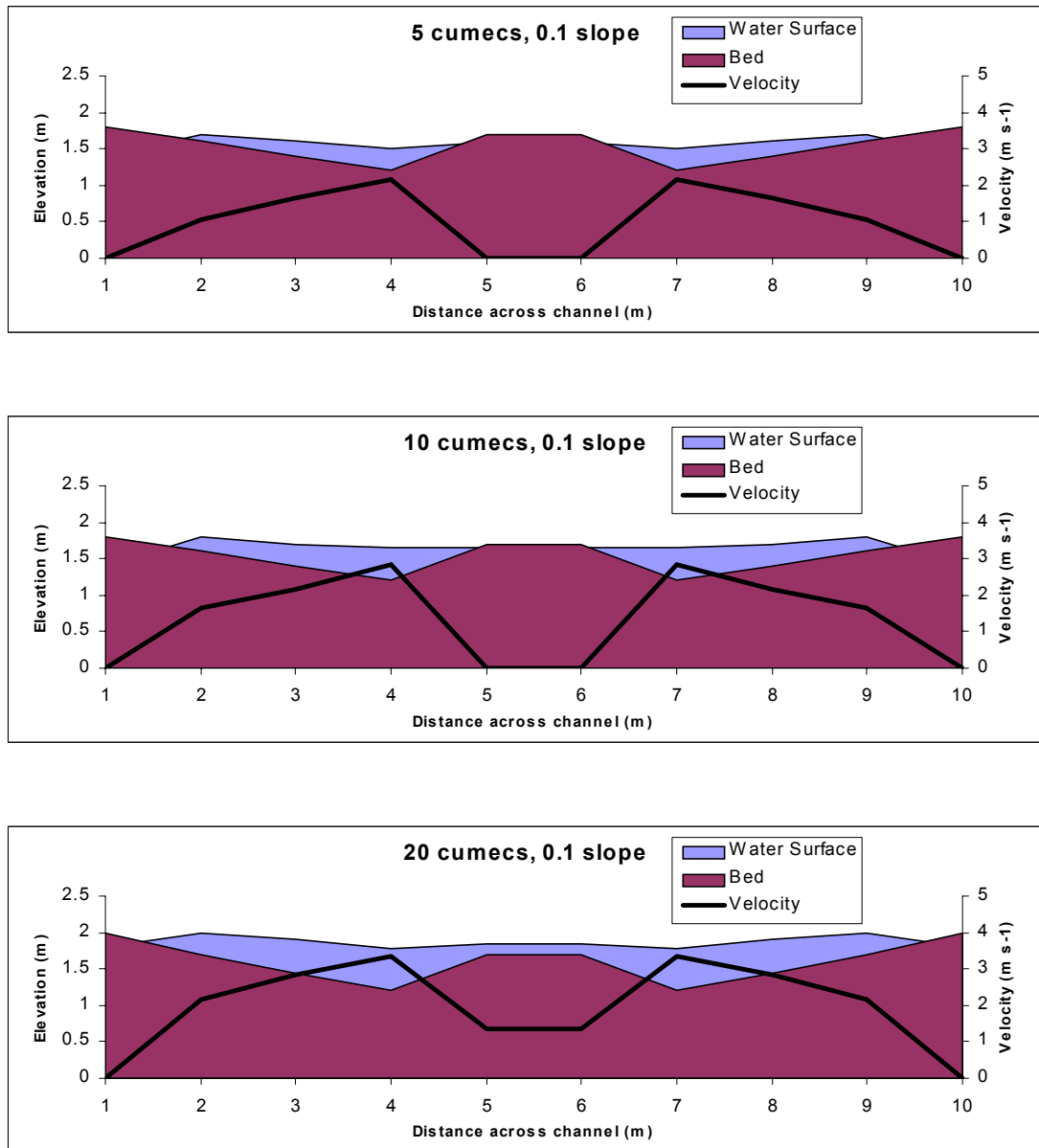


Figure 4.7. Velocity and water surface profiles for a triangular channel with central bar.

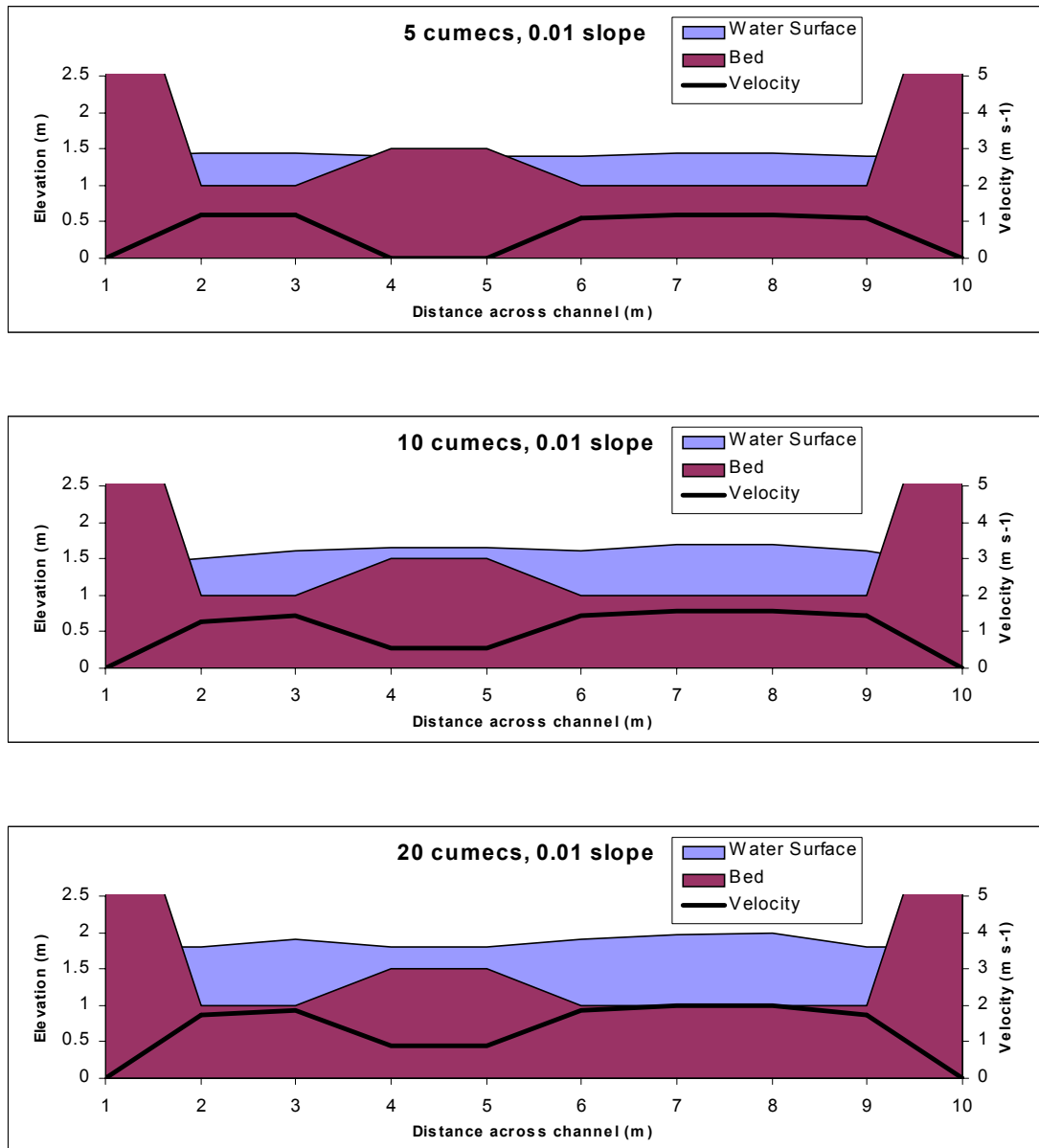


Figure 4.8. Velocity and water surface profiles in a rectangular channel with an off centre obstacle.

1. Manning's equation was developed from experimental data from open channel flow for cross section analysis. Despite the logical steps taken to convert it from a cross sectional formulae to operating over grid cells, sensitivity analysis shows that it is sensitive to changes in the hydraulic radius. This was probably the most difficult term to interpret when moving the equation to a CA format as it is difficult to transfer a cross section hydraulic radius to just one point. This may explain why the triangular channel gives a poor representation, as in a situation of changing depth, the hydraulic radius is a more variable term than in a rectangular channel. The simplification of setting the hydraulic radius equal to the depth is generally acceptable for a trapezoidal or rectangular channel. But for triangular, and parabolic cross sections R is closer to $2/3$ depth.
2. As noted previously, the slope calculation effects the surface profile. This is particularly evident in the triangular channel. In the example shown here, there is a side or lateral slope of 0.2, and the long profile slope is 0.1. If the model calculates the depth according to the average of the three downstream slopes, for the sides this means the depth is being over calculated, as the steepest lateral slope is ameliorated by the lower downstream slope. However, when compared with the discharge back calculated for the cross section, as in Figure 4.5, this performs better than using the steepest slope.
3. Water depth can be altered by changing the constant x in the routing equation (4.10) effecting the way water is distributed to its neighbours. Experimentation with this exponent shows that a value of less than 1 tends towards a concave cross channel profile whereas greater than 1 leads to a convex pattern. Murray and Paola (1994) use a similar exponent in their routing equation, and vary it between 1 and 0.5. They report that it appears to make little difference to their model.
4. The test channels are largely of unusual width-depth ratios and more importantly the model is unable to erode or deposit. If these functions are introduced the model rapidly changes the angular channel to a more rectangular shape. Also, with a narrow deep channel, incision and bank collapse would lead to a widening and reduction in depth, leading to a more appropriate width depth ratio.

These limitations must be placed in context. The model is not intended to emulate the more mathematically precise solutions offered by computational fluid dynamics, but aims to give a good representation of channel flow at a medium scale. The routing equations are widely used in GIS applications and hydrologic modelling (Desmet and Govers 1996, Murray and Paola 1994) and despite their simplicity still maintain a conservation of mass and direction of flow in the direction of maximum energy gradient, in this case the slope. By using Manning's equation for depth calculation, the flows and water levels produced may be inaccurate, but are not fundamentally wrong. The calculation of depth importantly allows flow over obstacles as well as around, and provides additional terms for use in the sediment transport laws used. Whilst accuracy is important, the depth precision is not as important as it may appear. A 20% inaccuracy in depth will only have a small effect on routing, as most of the time the flow is contained within the channel. Furthermore, with the depth slope relationship used in the Einstein equation, a 20% difference in slope (for example 0.01 to 0.012) between cells which may seem insignificant, would have the same effect as 20% difference in depth.

Importantly, the scanning routine seems to have little effect upon the water surface profiles. It was suspected that there would be a bias towards one side, depending as to the direction of the last scan. However, this does not show up on any of the surface profiles.

4.5.2 Testing of area calculation and scanning algorithm

As a dual test of the area calculation (3.2.2) and the scanning algorithm used for this and flow routing, the drainage area from the model was compared to one produced from the same DEM using ARC-INFO's FLOWACCUMULATION command. Table 4.1 shows the statistics produced for both sets and Figure 4.9 a visual comparison showing cells with a drainage area greater than 1500. All figures are in drainage units, a unit representing one grid cell. Therefore if a cell has a value of 1000, it drains 1000 grid cells, or drainage area is 1000 x grid cell area.

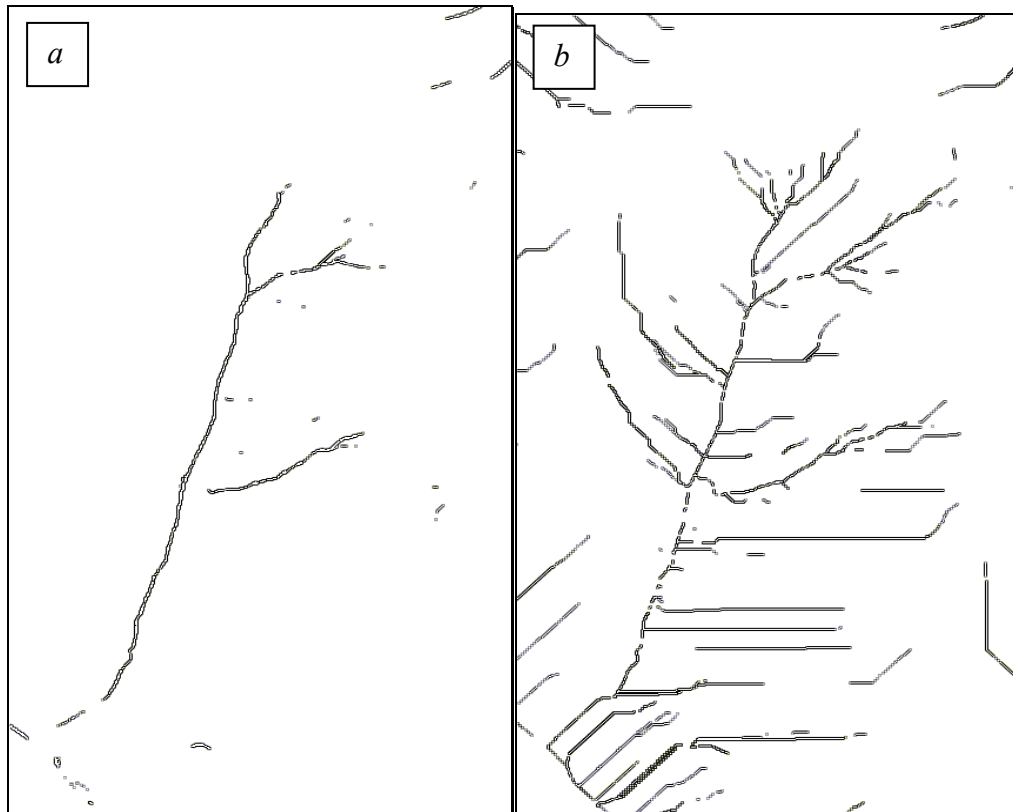


Figure 4.9. Drainage networks from the model (a) and ARC-INFO (b) all cells over 1500 drainage units.

	Model.	ARC-INFO
Maximum Value	373157	364527
Mean	339	323
Std Deviation	5973	5984

Table 4.1. Comparison between model and ARC-INFO drainage unit statistics.

Visually, differences between the two appear great, however ARC-INFO uses a single or steepest descent flow routine whereas the model uses a multiple flow algorithm as discussed in section 3.1.5. The single flow method does not allow divergent flow, concentrating the drainage area into channels. In the model, use of a multiple flow routing method allows flow to diverge across the hillslopes instead of being forced to accumulate in single threads, so that the model only picks up the main channel network. This is further compounded by the use of the initial DEM with its smooth interpolated valley floors which allow the easy divergence and spread of flow. Table 4.1 possibly represents the best comparison, with the means and standard deviations of both methods very similar.

4.5.3 Grid cell size validation

Section 3.1.5 discusses the importance of grid cell size, and the choice of grid cell size is thought to have a large effect on the performance of the model. To test this sensitivity, the same initial conditions were taken and using the RESAMPLE command in ARC-INFO, the 1m grid was re-sampled to 1.4, 2, 3, and 4 metre resolution. The model was run from the bare initial conditions (section 4.4.1) with a high sediment supply, for 50 000 minutes, using the hourly rainfall data (section 5.4, Figure 5.9 and Figure 5.10) which included two small floods. The sediment discharge from all runs was noted.

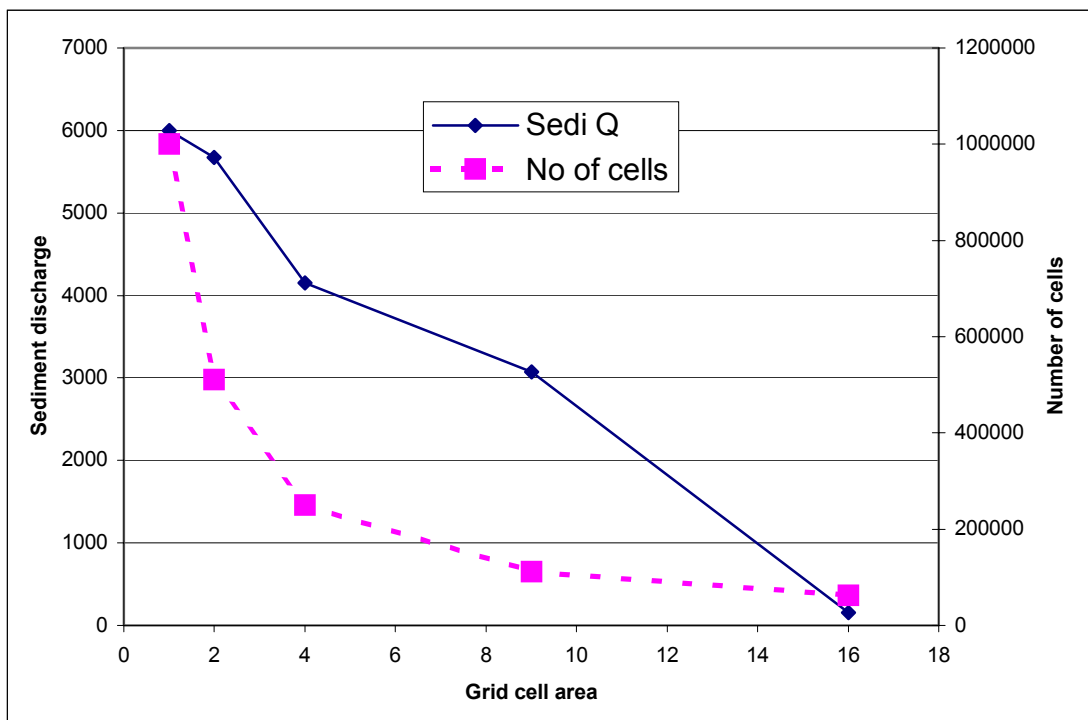


Figure 4.10. Changes in sediment discharge and number of grid cells with grid cell area.

Figure 4.10 shows a steady decrease in sediment discharge with increase in grid cell area, with a rapid drop above 9m^2 down to 150, suggesting a threshold around that size. This may be caused by a reduction in local flow concentration from which erosion is initiated. Further examination shows a decrease in physical detail (for example channel bank deposits) with an increase in cell size. However, the general form and location of such detail remains the same.

As model speed is directly related to the number of grid cells, the choice of grid cell size represents an important compromise between accuracy and speed. Figure 4.10 suggests an ideal resolution of between 2 and 3m³ as having least cells, but without too great a drop in sediment discharge. However, if the grid size is too great, then we are faced with the issue of running with grid cell size potentially larger than the stream. The issue is further complicated by the large spatial scale range over which the processes operate. For example, a large landslide is unlikely to be effected by a large grid cell size, whereas the formation of a bar will be swallowed up within a large cell.

4.5.4 'Other' parameters

Many of the parameters discussed in this chapter have not been tested *per se*, but have been investigated to some extent during the lengthy development of the model. It is likely that many of these can never be accurately assessed due to the large spatial extent of the model and numerous interdependencies and feedbacks.

4.6 Conclusions

The CA methodology has allowed the specifications outlined in section 4.1 to be attained. The scanning method and optimisations of sections 4.2.3 and 4.3.2 enable the whole basin to be modelled. Within the catchment model, there is a detailed representation of fluvial erosion and deposition for nine grainsize fractions, preserving a stratigraphy through a further ten active layers. Slope processes of soil creep and mass movement are applied, as are the effects of vegetation on both the hydrology and surface strength. Furthermore, the set-up described in this chapter is only one example. The program is structured so it can be tailored to a variety of applications by altering the grainsizes, vegetation factors, adding extra active layers, grid cell size etc.

However, the model is far from perfect. Validation of results will inevitably be difficult as the model generates more data than we can measure in the field. The complexity of the model and non linear behaviour (Chapter 9) can create many problems, and whichever sediment transport laws used are only based upon regression analysis from a few field sites. The hydraulic approximations are potentially inaccurate (section 4.5.1.2) and the novel scanning algorithm is untested outside of this work.

But the model's results must be taken in context of the size and scale of the basin modelled. Given current computing power, high resolution CFD models cannot be applied to a large channel network, and there are fundamental problems associated with integrating sediment transport and other factors within these. Therefore this model represents an attempt to model an entire catchment at the highest possible scale over a long period. The results cannot be expected to be completely accurate (as no models will ever be) but provide a good representation of the processes and feedbacks operating within the catchment. The accuracy here is relative, and the true success or failure of this modelling scheme will be demonstrated by what we learn from it, principally the relative importance and effects of different types of environmental change upon a catchment.